J. Ind. Eng. Chem., Vol. 13, No. 5, (2007) 827-834

Biological Toxicity Toward Zebrafish (*Danio rerio*) of Na- and K-TiO_2 Photocatalytic Systems During the Decomposition of Bisphenol A

Min-Kyu Jeon, Min-Kyeong Yeo, Hyung-Joo Choi, Jinsoo Kim, Suk-Jin Choung, Jin-Bae Kim*, Daewon Jeong, and Misook Kang***, †**

College of Environmental and Applied Chemistry, KyungHee University, Yongin, Gyeonggi 449-701, Korea
**Department of Chemical Engineering, Hoseo University, Asan, 336-795, Korea*
***Department of Microbiology and Aging-associated Disease Research Center, Yeungnam University college of Medicin, Daegu 705-717, Korea*
****Department of Chemistry, College of Science, Yeungnam University, Gyeongsan, Gyeongbuk 712-749, Korea*

Received March 19, 2007; Accepted June 1, 2007

Abstract: In this study we examined the alkali metal-TiO_2 photocatalytic decomposition of bisphenol A (BPA) and its biological toxicity to Zebrafish (*Danio rerio*). Alkali metal-TiO_2 particles, which were prepared using a common sol-gel method, were used in an attempt to decompose BPA at a concentration of 10.0 ppm. The alkali metal-TiO_2 particles having an anatase structure were ca. 50～100 nm in size and had surface areas of ca. 14～24 m^2/g. BPA, at a concentration of 10 ppm, was completely degraded by K-TiO_2 photocatalysis after 50 h. However, 3.0 and 2.5 ppm BPA remained after 50 h when using pure TiO_2 and Na-TiO_2, respectively. A decrease in survival rate was observed for Zebrafish that had been reared in water containing 0.1 ppm BPA. Before photocatalysis, there were no toxic effects on the hatching rates or morphogenesis of the Zebrafish observed when using any of the photocatalyst powders, except for the pure TiO_2 powders. Surprisingly, the pure TiO_2 powder affected the Zebrafish: the hatching rates were remarkably lower than they were when using Na-TiO_2 and K-TiO_2 as the photocatalyst powders. During photocatalysis of 0.1 ppm BPA, serious toxic effects on the hatching rates or morphogenesis of Zebrafish were observed for each of the photocatalyst powders used. However, no toxicity was observed after BPA had been completely decomposed by the alkali metal-TiO_2 photocatalysts.

Keywords: *alkali metal-TiO_2 powder, bisphenol A (BPA), photodecomposition, biological toxicity, zebrafish*

Introduction

[1)]

Bisphenol A (BPA) is manufactured in high quantities, with over 90 % being used as a monomer for the production of polycarbonate and epoxy resins, unsaturated polyester-styrene resins, and flame retardants.

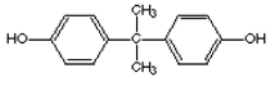

Bisphenol A

The final products are used as coating for cans, in powdered paints, as additives in thermal paper, in dental fillings, and as antioxidants in plastics [1]. BPA has estrogenic activity and is considered to be an environmental endocrine disrupter [2]. Moreover, BPA has been reported to leach from polycarbonate baby bottles [3], reusable containers [4], and drinking water tanks [5]. BPA has also been detected in plastic waste [6], in plasma stored in polycarbonate tubes [1], and in aquatic environments [7]. High BPA concentrations can also be found in wastewater from BPA production factories, because it is only partially removed during wastewater treatment, and can be a source of contamination in aquatic environments [7]. Although BPA is readily degraded by microorgan-

† To whom all correspondence should be addressed.
(e-mail: mskang@ynu.ac.kr)

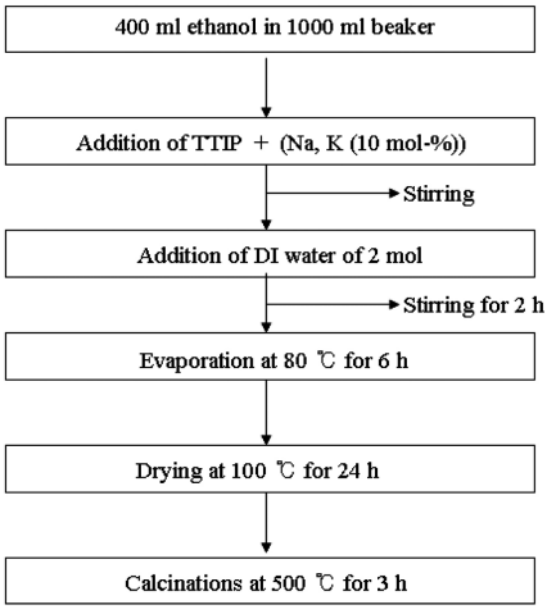

Figure 1. Preparation of the TiO_2, Na-TiO_2, and K-TiO_2 particles using a conventional sol-gel method.

isms [1], biological methods generally require long treatment times for treating wastewater containing BPA in high concentrations. Therefore, a rapid and simple method of wastewater treatment for BPA is urgently required. A variety of techniques involving chemical [8], biological [9,10], photochemical [11], and electrochemical [12] procedures have been examined for the treatment of wastewater containing phenolic compounds.

In recent years, several studies have reported the application of TiO_2 to biology. The disinfection behavior on a photo-excited TiO_2 surface and the disinfection effect of photo-excited TiO_2 have been described [13,14]. The effective removal or inactivation of pathogenic organisms through disinfection is the most important process in the treatment and distribution of drinking water. The most common means of disinfecting potable water is through the use of chlorine. However, chlorination results in the production of low-molecular-weight, halogenic organic compounds, which are collectively termed "sterilization byproducts." Although chlorinated water is generally free of pathogenic microorganisms, many of the sterilization byproducts can have adverse effects on human health over the course of a lifetime. Therefore, there has been an intensive search for alternative water-treatment practices that not only maintain or improve the current levels of microbiological safety but also reduce or eliminate chemical byproducts resulting from the oxidation process.

Recently, several researchers [8,11,15] have reported the treatment of wastewater containing BPA. They examined the degradation of BPA in the presence of TiO_2 as a photocatalyst. However, there is little data on the toxicology during TiO_2 photocatalysis [16,17]. In a previous study [18], we reported that the biology of Zebrafish was not affected by TiO_2 photocatalysts, although we had only focused on using film-type photocatalysts. However, many studies into the decomposition of environmental pollutantsn have used powder types photocatalysts. In these cases, the organisms examined were exposed to the ultra-fine photocatalyst particles. Consequently, the skin surface of an organism may be surrounded by many fine particles, which the organism might swallow during feeding. Therefore, the hatching rate and morphology of an organism when the organism consumes fine photocatalysts powders should be tested before applying a photocatalyst powder to disinfection or environmental remediation.

In this study, alkali metal (Na, K)-incorporated TiO_2 photocatalysts, which were prepared to increase the concentration of OH radicals, were used to decompose BPA (10 ppm), and the biological toxicity to Zebrafish (*Danio rerio*) was examined before, during, and after the photoreaction. In addition, instead of a film, nanometer-sized alkali metal-TiO_2 powders were used to determine the biological toxicity.

Experimental

Catalyst Preparation

Figure 1 shows the methodology used to prepare the alkali metal (Na, K)-TiO_2 photocatalysts using a conventional sol-gel method. The reagents used were as follows: titanium tetraisopropoxide (99.95 %, TTIP, Junsei Chemical, Japan), NaOH (99.9 %, Junsei Chemical, Japan), and KOH (99.95 %, Junsei Chemical, Japan) as the titanium dioxide, sodium oxide, and potassium oxide precursors, respectively. The concentrations of Na and K were fixed at 10 mol-% per TTIP in the initial solution. Ethanol (99.9 %, Wako Pure Chem. Ltd.) was used as the solvent for hydrolysis. A mixture of 0.1 mol alkali and 1.0 mol TTIP precursors, 0.25 mL of nitric acid (35 %, Junsei Chemical Co. Ltd., Japan), and 100 mL of ethanol was stirred until a homogeneous gel had formed. The solvent was evaporated at 80 ^{o}C for 6 h. The precipitate was dried and calcined at 100 ^{o}C for 24 h and then at 500 ^{o}C for 3 h.

Catalyst Characterization

The prepared alkali metal-TiO_2 powders were analyzed by powder X-ray diffraction (XRD, model PW 1830, Philips) with nickel-filtered Cu*Ka* radiation (30 kV, 60 mA) at angles from 5 to 70^{o}. The scan speed was 10 ^{o}/min, and the time constant was 1 s. A diffraction angle (2θ) of 25.0^{o} (101 plane) was selected to determine the crystalline structure of the sample.

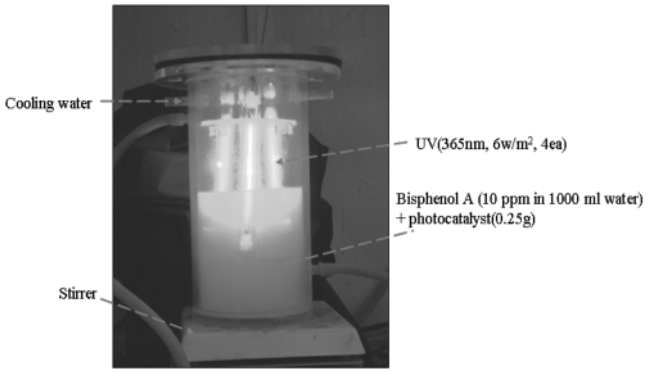

Figure 2. Photocatalytic reactor for Bisphenol A decomposition.

The particle sizes and shapes of the alkali metal-TiO_2 powders were observed by scanning electron microscopy (SEM or FESEM, model JEOL-JSM35CF). The power was set at 15 kV. The BET surface area of the sample and pore size distributions (PSD) were measured through nitrogen gas adsorption using a chromatograph equipped with a TCD detector at liquid nitrogen temperature. A mixture of nitrogen and helium as the carrier gas was flowed using a GEMINI2375 instrument (Micrometrics). The sample was thermally treated at 350 °C for 3 h before measuring the level of nitrogen adsorption.

At this point, XPS peaks could be identified using the tabulated binding energy values from the XPS handbook, yielding information on the chemical composition and bonding environment. The XPS spectra were acquired using an ESCA 2000 instrument. The spectra, which were generated by AlKα X-rays (15 kV, 350 W), were collected for 20～90 min, depending on the peak intensities, at an energy of 23.5 eV.

Photodecomposition of Bisphenol A

The decomposition of BPA (97 %, Sigma-Aldrich, Korea) was carried out using a general stationary closed apparatus, as shown in Figure 2. The BPA concentration was fixed at 10 ppm. First, BPA was dissolved at a concentration at 10 ppm in water containing 0.5 mL of methanol (99 %, Merck) and then diluted by 1 liter aqueous solution. The alkali metal-TiO_2 colloidal solutions were used directly for the BPA photodecomposition reaction. The UV lamps (model UV-A, 365 nm, 6 W × 4 ea, 20 cm length × 1.5 cm diameter, Shinan Co., Korea) were equipped with a photocatalytic liquid system. The amount of photocatalyst used was 0.25 g/1000 mL. Analyses of the BPA concentration in the reaction solution before and after the reaction were carried out using UV-visible spectroscopy (Shimadzu MPS-2000 spectrometer) and HPLC using the following conditions: column, C_{18} column; mobile phase, acetonitrile, water (6:5, v/v); flow rate, 0.7 mL/min; detector, UV 275 nm. To test the toxicity to Zebrafish, the BPA concentration was set to 0.1 ppm/1000 mL water, and 0.2 g of the photocatalysts powders were injected into the solution.

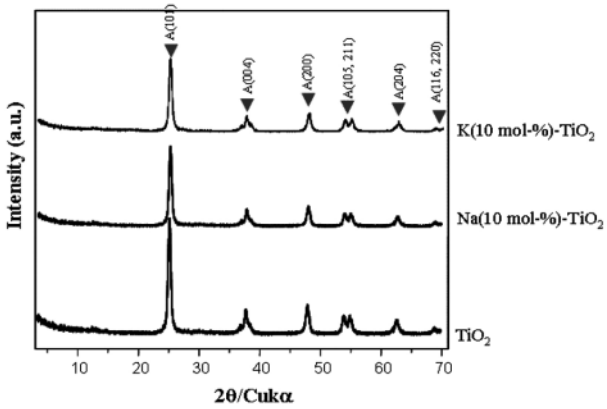

Figure 3. XRD patterns of TiO_2, Na-TiO_2, and K-TiO_2 particles after calcination at 500 °C for 3 h.

Treatment of Embryos to Observe the Developmental Stages

The effect of the alkali metal-photodegradation on the hatching rate of the Zebrafish embryos was assessed as described previously [19]. Zebrafish (3～5 months old) were purchased from the Kangnam Aquarium (Suwon, Korea). The general care of the adults and embryos was carried out according to the report by Westerfield [20]. Briefly, the wild-type Zebrafish from a colony established at KyungHee University by Prof. Yeo were held in 60-L glass tanks and maintained in a carbon-filtered water system at 28 ± 1 °C under a 14 h photo period. The adult fish were fed blood worms, dry flake food, and/or brine shrimp. The eggs were laid and fertilized within 1 h of the beginning of the light cycle, which provided large populations of synchronously developing embryos.

The embryos were collected, pooled, and rinsed several times. Embryonic staging was carried out according to the standardized staging series reported by Kimmel et al. [21]. The embryos were immersed in the exposure or vehicle control solutions beginning at 64- to 256-cell stages, 22.5 h after fertilization (hpf). The dead embryos were removed to prevent contamination of the test solutions. The embryos were observed using a Leica Letiz Biomed microscope to determine the morphological effects.

Results and Discussion

Characterization of the Alkali Metal-TiO_2 Photocatalysts

Figure 3 shows the XRD patterns of the alkali metal-TiO_2 photocatalysts. The alkali metal-TiO_2 produced a sharp peak at 25.0°(101), which is the major characteristic peak for anatase. All other peaks were attributed to

Table 1. Physical Properties of the TiO_2, Na-TiO_2, and K-TiO_2 Particles

Catalyst	Composition on surface (Atomic %)			Average pore size (Å	Average pore volume (mL/g)	Surface area (m^2/g)	Zeta-potential in distilled water (mA)
	Na, K	Ti	O				
TiO_2	-	38.03	61.97	56.6	0.039	14.3	+24.0
Na (10 mol%)-TiO_2	2.69	36.35	60.96	93.3	0.084	24.3	-38.5
K (10 mol%)-TiO_2	0.54	14.84	84.62	58.9	0.035	14.7	-41.5

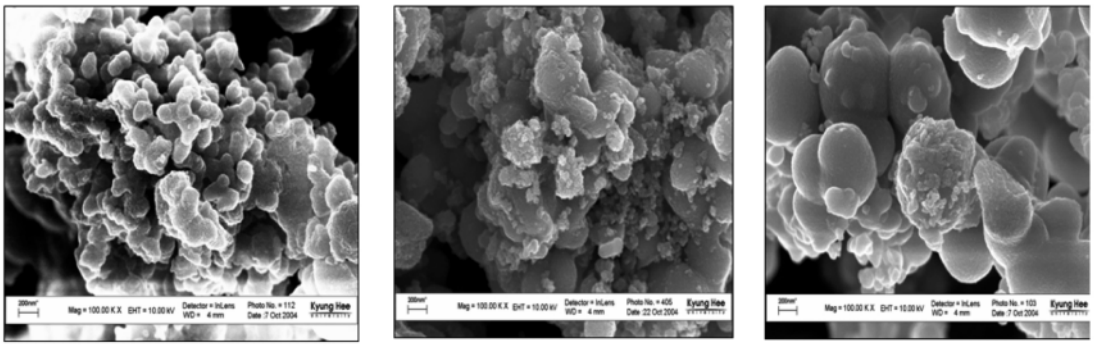

Figure 4. SEM images of TiO_2, Na-TiO_2, and K-TiO_2 particles after calcination at 500 °C for 3 h.

the common anatase structure of the powder type in this study. The most commonly used phases of TiO_2 are rutile and anatase. Anatase is more useful as a photocatalyst than rutile owing to its higher photoactivity. However, the source of the difference in activity is unknown. In particular, mixtures of anatase and rutile (e.g., Degussa P-25, which consists of ca. 80 % anatase and 20 % rutile) show better photoactivity than do either of the phases alone.

Figure 4 shows SEM images of the alkali metal-TiO_2 powders. The particles were spherical and ca. 50～100 nm in size. The particle size increased with incorporation of the alkali metals.

Table 1 summarizes the physical properties of the catalysts. The real composition on the surface, which was determined using EDAX, was generally lower than the amount of precursor added in the sol preparation. In particular, with an addition of potassium, the decrease was more remarkable compared with that of sodium. The Table also gives the pore volumes and pore diameters. Bulk pores between the particles of ca. 20.0 Å were generated when sodium was added to the titanium site. The pore volume also increased after the addition of sodium, which corresponded to the measured BET surface areas. However, the surface areas were very small for all samples, < 25.0 m^2/g.

The Zeta potential is a term commonly used in colloidal chemistry. When a tiny mineral or organic particle is suspended in a fluid, the Zeta Potential maintains the dispersion or discreteness of the particles in suspension. It is well known that like charges repel and opposite charges attract. In an ideal system, all particulates should have the same electrical charge. If the particles have no electrical charge, they can agglomerate and precipitate. Therefore, a high Zeta Potential indicates a better dispersion of particles. A high Zeta Potential or negative electrical charge on the particles may help to increase the dispersion or discreteness of the particles in water. In Table 1, the Zeta potentials of TiO_2, Na-TiO_2, and K-TiO_2 in distilled water were +24, -38.5, and -41.5 mA, respectively. Thus, means that the surface stabilization and dispersion of alkali metal-TiO_2 in a photocatalytic liquid system was more enhanced compared with that of the pure TiO_2. In addition, the surface charges of the TiO_2 photocatalysts can be changed by the addition of alkali metal.

Quantitative XPS analysis was performed on the TiO_2 and alkali metal-TiO_2 particles. Figure 5 shows typical survey and high-resolution spectra. The survey spectra of the TiO_2 and alkali metal-TiO_2 particles contained Ti 2p and O 1s peaks from TiO_2. The Ti 2p1/2 and Ti 2p3/2 spin-orbital splitting photoelectrons for all samples were located at binding energies of 465.0 and 458.3 eV, respectively. The binding energy decreased after the addition of the alkali metal. In general, an increase in binding energy means an increase in the oxidation state of the metal. Therefore, the titanium oxidation state in alkali metal-TiO_2 (Ti^{3+}) was lower than that in pure TiO_2. The activity of a photocatalyst is closely related to the Ti oxidation state: Ti^{3+} ions are more effective photocatalysts. The Gaussian values were used in the curve resolution of the individual O 1s peaks (first peak O1: 530.0 eV; sec-

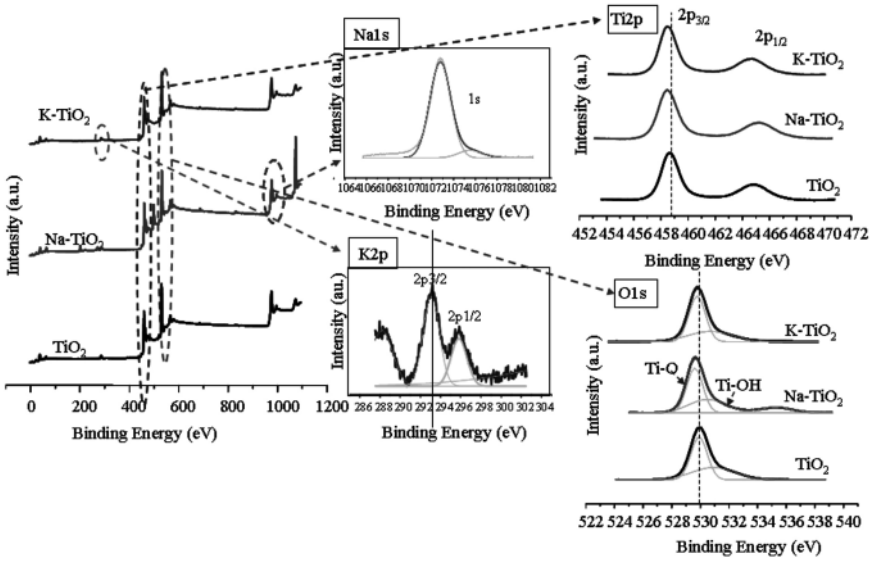

Figure 5. XPS curves of TiO_2, Na-TiO_2, and K-TiO_2 particles after calcination at 500 °C for 3 h.

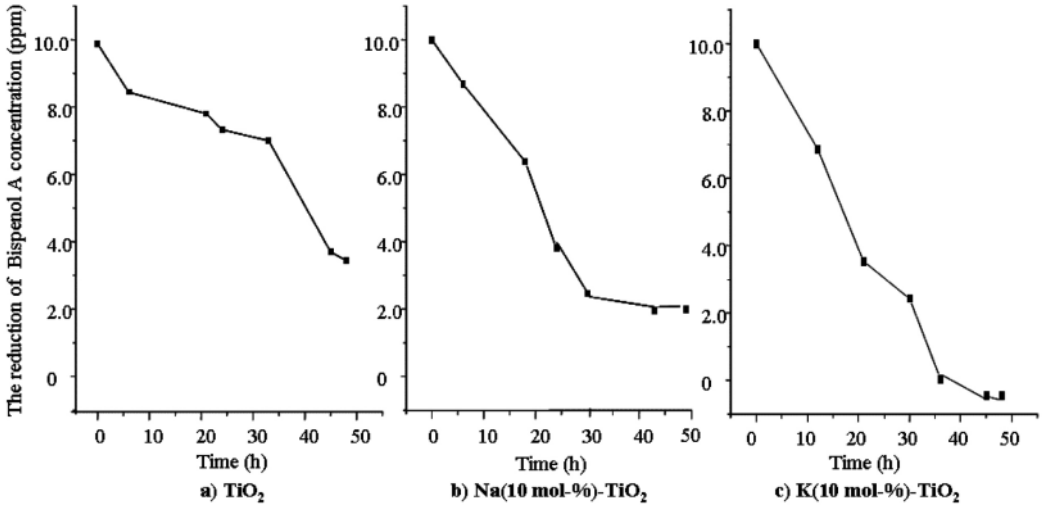

Figure 6. Bisphenol A photodecomposition on TiO_2, Na-TiO_2, and K-TiO_2 particles.

ond peak O2: 532.0 eV) in the two spectra. The two curve-resolved O 1s signals were assigned to Ti^{4+}-O and Ti^{3+}-O, respectively. The locations of the binding energies for the second peaks agree well with the reported values for the bulk oxide (O^{2-}) and the hydroxyl (OH) species. In general, a large peak indicates a high hydrophilicity. However, the peak areas and widths were similar in all samples. On the other hand, a 1s peak at 1071.5 eV and two peaks at 293.1 and 296.0 eV were assigned to the 1s energy of Na metal and the 2p3/2 and 2p1/2 energies of K metal in the TiO_2 framework, respectively.

Photodecomposition of Bisphenol A

Figure 6 gives a comparison of the various BPA photodecompositions. Decomposition barely occurred when bubbling air at a rate of 500 mL/min/UV-A radiation (wavelength > 365 nm). The BPA was completely decomposed in the UV-A radiation/air bubbling/K-TiO_2 photocatalytic system after 48 h. However, 3.0 and 2.5 ppm BPA still remained in the pure TiO_2 and Na-TiO_2 systems, respectively. In particular, in the initial stages, the rate of BPA decomposition on alkali metal-TiO_2 increased, while the rate was very slow on pure TiO_2. This result might be due to the surface properties of the photocatalysts, such as their Zeta potentials.

Figure 7 shows the change in pH of the water during the photodecomposition of (10 ppm) BPA. In non-photocatalysis, the pH in a photocatalyst colloidal solution was not the same in all samples: the pure TiO_2 and alkali metal-TiO_2 colloidal solutions had weak acidity (pH = 6.0) and alkalinity (pH = 7.1～7.4), respectively. This situation might be related to the surface charge of the zeta

Table 2. Effect of Alkali-Metal-TiO_2 Photodegradation on the Hatching Rate of Zebrafish Embryos

Conditions	Hatched rate % (number of hatched embryos/number of unhatched embryos) with UV radiation	Hatched rate % (number of hatched embryos/number of unhatched embryos) with UV radiation
Base group	3.75 % (6/160)	85.5 % (171/200)
TiO_2, 0.025 g/L	1.25 % (2/160)	40.5 % (81/200)
TNa-TiO_2, 0.025 g/L	2.50 % (4/160)	89.0 % (178/200)
K-TiO_2, 0.025 g/L	6.25 % (10/160)	88.0 % (176/200)

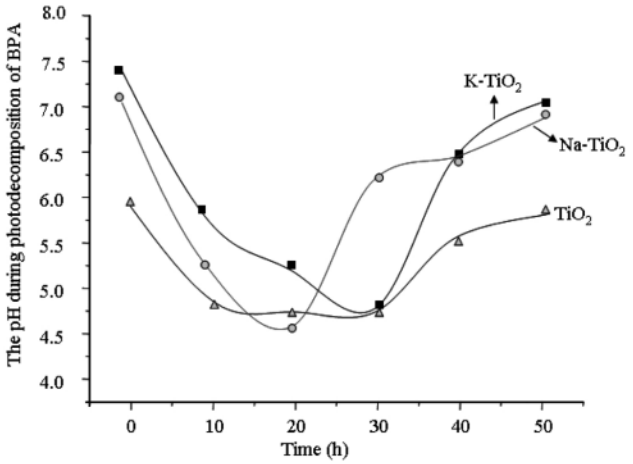

Figure 7. Changes in pH during Bisphenol A photodecomposition on TiO_2, Na-TiO_2, and K-TiO_2 particles.

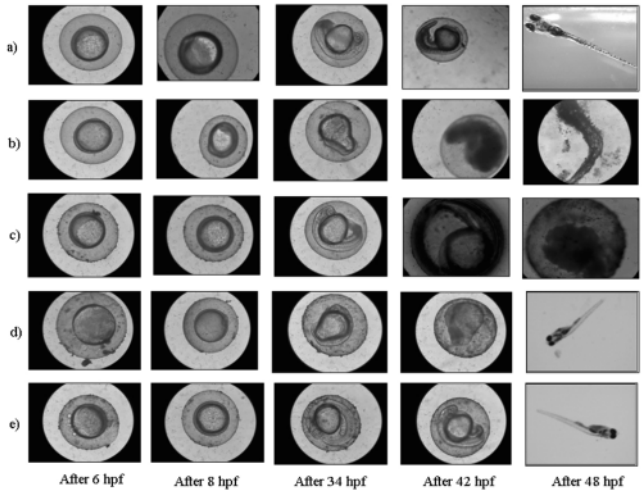

Figure 8. Morphogenesis of the untreated zebrafish embryos in the control group and the morphogenesis of zebrafish according to various conditions before photocatalysis: a) control group, b) under UV-A irradiation, c) with TiO_2 particles without irradiation, d) with Na-TiO_2 particles without irradiation, and e) with K-TiO_2 particles without irradiation.

potential: the pure TiO_2 and alkali metal-TiO_2 had positive and negative charges, respectively. On the other hand, during photocatalysis, the pH in the photocatalytic systems become acidic as a result of the increase in the concentration of H^+ generated from the decomposition of BPA. However, the pH returned to the initial value after the decomposition of BPA. Figures 6 and 7 show that the photodecomposition of BPA can be enhanced by adding an alkali metal into the TiO_2 framework.

Toxicity to Zebrafish Before and During Photocatalysis

Figure 8 shows the morphogenesis of Zebrafish according to the hpf (hour post-fertilization) prior to photocatalysis. In the control group, the hatched Zebrafish fry was seen after 46 h. However, an enlarged pericardium was not observed in the hatched fry of the few eggs exposed to UV-A radiation (Figure 8b). This result shows that UV irradiation, even though a weak energy, significantly affected the Zebrafish hatchings. This result suggests that the effect on the hatching rate is increased during early developmental stages as a result of protein damage from UV-A radiation. On the other hand, the growth of embryogenesis of Zebrafish was also affected when the Zebrafish embryos were exposed to the photocatalyst fine powders without UV-A irradiation. TiO_2 was believed to be relatively inert to organisms. However, this study showed that fine powders having positively charged surfaces, which induced coagulation, could depress the growth of Zebrafish embryos. Simultaneously, the hatching rate in the presence of TiO_2 powders was lower than that of the controls (Table 2). On the other hand, in the case of the alkali metal-TiO_2, embryogenesis under non-UV-A irradiation was normal, and no morphological changes in the Zebrafish embryos were observed.

Figure 9 shows the embryogenesis of Zebrafish during photocatalysis. First, in the presence of 0.1 mol BPA, the embryos showed no growth until 48 h. This result shows that BPA affects the developing Zebrafish both before and during photocatalysis. In particular, embryogenesis was stopped after exposure to BPA/TiO_2/UV-A irradiation during photocatalysis, and the embryos were more disrupted (Figure 9b). Simultaneously, the hatching rate during TiO_2 photocatalysis was lower than those observed before photocatalysis of the other samples (Table 2). These results suggest that the effect on the hatching rate is induced by protein damage under UV-A irradiation/ BPA/TiO_2 during the early developmental stages. In addition, Zebrafish showed morphological and devel-

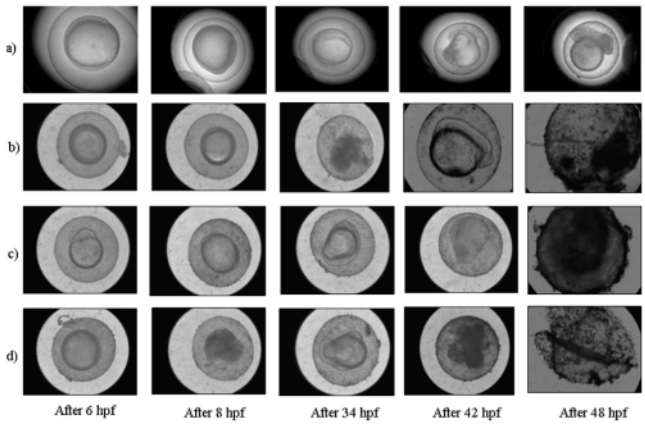

Figure 9. Morphogenesis of zebrafish according to hpf during photocatalysis. a) With BPA (0.1 mol) b) during TiO_2 photocatalysis, c) during Na-TiO_2 photocatalysis, and d) during K-TiO_2 photocatalysis.

opmental toxicity during alkali metal-TiO_2 photocatalysis, but the hatching rates were higher than that of pure TiO_2 photocatalysis (Table 2). These results show that the photodegradation of BPA can be enhanced using alkali metal-TiO_2 and that the toxicity to the organism also can be depressed. In addition, the toxicity disappeared after the BPA had been completely decomposed by Na- and K-TiO_2 photocatalysis, and the Zebrafish were still living after 6 months.

Table 2 summarizes the hatch rate percentage of Zebrafish before and during photocatalysis. The data is expressed as the mean ± SEM of the embryo groups. Significant differences compared with the corresponding controls are indicated with an asterisk ($P < 0.05$). In this study, almost all the eggs that had been exposed solely to BPA (0.1 mol) failed to hatch, which was attributed to the presence of the eluted BPA, which affected the early, sensitive stages of embryonic development. During UV-irradiation, the hatch rates decreased remarkably. On the other hand, the hatch rate was also decreased by the presence of TiO_2 particles, but it improved in the presence of alkali metal-TiO_2. In addition, the hatching rate of the eggs exposed to BPA and the TiO_2 photocatalysis for 48 h during photocatalysis was lower than those exposed to the alkali metal-photocatalystic systems. This situation arose because the photocatalysis affected the Zebrafish while promoting BPA decomposition. These results show that BPA, UV-radiation, and pure TiO_2 photocatalyst powders competitively affect the developing Zebrafish both before and during photocatalysis.

Conclusion

TiO_2 and two alkali metal-TiO_2 photocatalysts were used to decompose BPA, and their biological toxicity to Zebrafish was investigated before and during the photoreaction. The photocatalysts were used as powders in the BPA photodecomposition system. BPA at a concentration of 10 ppm was completely degraded by the K-TiO_2 photocatalysis after 50 h, but 3.0 and 2.5 ppm BPA still remained after 50 h when pure TiO_2 and Na-TiO_2 were used. Zebrafish embryos reared in water exposed to pure TiO_2 had a lower survival rate. However, no adverse effects on the hatching rates and morphogenesis of Zebrafish were observed when the Zebrafish embryos were exposed by Na- and K-TiO_2. On the other hand, toxicity during BPA photocatalysis was observed in all of the samples, but there was no toxicity after the BPA had been completely decomposed by the Na- and K-TiO_2 photocatalysts. Overall, alkali metal-TiO_2 photocatalysts can enhance the decomposition of BPA with relatively low toxicity to an organism.

Acknowledgment

This work was also partially supported by a grant (R13-2005-005-01004-0) from the Korea Science and Engineering Foundation (KOSEF) to the Aging-associated Vascular Disease Research Center at Yeungnam University.

References

1. C. A. Staples, P. B. Dorn, G. M. Klecka, S. T. O'Block, D. R. Branson, and L. R. Harris, *Chemosphere* **36**, 2149 (1998).
2. A. V. Krishnan, P. Stathis, S. F. Permuth, L. Yokes, D. Freldman, and N. Sonoyama, *Endocrinology* **132**, 2279 (1993).
3. Y. Sun, M. Wada, O. A. Dirbashi, N. Kuroda, H. Nakazawa, and K. Nakashima, *J. Chromatogr.* B, **749**, 49 (2000).
4. J. E. Biles, T. P. McNeal, T. H. Begley, and H. C. Hollifield, *J. Agric. Food. Chem*., **45**, 3541 (1997).
5. B. Bae, H. Choi, M. S. Lim, N. Y. Lee, and N. Y. Chang, *J. Korean Soc. Water Wastewater*, Seminar D-10 (2000).
6. T. Yamamoto and A. Yasuhara, *Chemosphere* **38**, 2569 (1999).
7. J. Sajiki, K. Takahashi, and J. Yonekubo, *J. Chromatogr. B*, **736**, 255 (1999).
8. N. Watanabe, S. Horikoshi, H. Kawabe, Y. Sugie, J. Zhao, and H. Hidaka, *Chemosphere* **52**, 851 (2003).
9. J. Q. Jiang, Q. Yin, J. L. Zhou, and P. Pearce, *Chemosphere*, **61**, 544 (2005).
10. S. Aguayo, M. J. Muoz, A. Torre, J. Roset, E. Pea, and M. Carballo, *Sci. Total Environ*., **328**, 69 (2004).

11. S. B. Kim, G, S. Kim, and S. C. Hong, *J. Ind. Eng. Chem.*, **12**, 749 (2006).
12. S. Tanaka, Y. Nakata, H. Kuramitz, and M. Kawasaki, *Chem. Lett.* 943 (1999).
13. J. H. Lee, M. Kang, S.-J. Choung, K. Ogino, S. Miyata, K. J. Yoon, M.-S. Kim, and J. Y. Park, *Water Res.*, **38**, 713 (2004).
14. M. S. Lee, J. D. Lee, and S. S. Hong, *J. Ind. Eng. Chem.*, **11**, 4, 495 (2005).
15. Y. Ohko, I. Ando, C. Niwa, T. Tatsuma, T. Yamamura, T. Nakashiuma, Y. Kubota, and A. Fujishima, *Environ. Sci. Technol*., **35**, 2365 (2001).
16. B. Kim, *Chemosphere*, **52**, 277 (2003).
17. D. D. Sun, *Water Res*., **37**, 3452 (2003).
18. M. K. Yeo and M. Kang, *Water Res*., **40**, 1906 (2006) .
19. M. K. Yeo, *Korean J. Environ. Health*, **29**, 1 (2003).
20. M. Westerfield, *The Zebrafish Book: A Guide for the Laboratory Use of Zebrafish*, University of Oregon Press, Eugene, Oregon (1995).
21. W. Kimmel, S. Ballard, B. K. Ullman, and T. Schilling, *Developmental Dynamics*, **203**, 253 (1995).